

# Evaluation of trabecular structure of hamate using micro-computed tomography

Hakan Ocak<sup>1</sup> , Hakan Hamdi Çelik<sup>2</sup> , Mert Ocak<sup>3</sup> , Ferhat Geneci<sup>4</sup> 

<sup>1</sup>Department of Anatomy, Faculty of Medicine, Ağrı İbrahim Çeçen University, Ağrı, Türkiye

<sup>2</sup>Department of Anatomy, Faculty of Medicine, Hacettepe University, Ankara, Türkiye

<sup>3</sup>Department of Anatomy, Faculty of Dentistry, Ankara University, Ankara, Türkiye

<sup>4</sup>Department of Anatomy, Faculty of Medicine, Ankara Yıldırım Beyazıt University, Ankara, Türkiye

## Abstract

**Objectives:** In this study, we intended to reveal the trabecular structure of hamate by using micro-computed tomography.

**Methods:** This study was carried out on 55 human dry hamates. The bones were scanned with a micro-CT device. Volume, surface, and trabecular parameters (trabecular number, trabecular thickness, trabecular separation) of the scanned bones were analyzed.

**Results:** The mean percentage of the bone volume was  $44.930 \pm 5.859\%$ , trabecular number was  $1.31 \pm 0.150 \text{ mm}^{-1}$ , trabecular thickness was  $0.35 \pm 0.056 \text{ mm}$ , trabecular separation was  $0.57 \pm 0.087 \text{ mm}$ .

**Conclusion:** Hamate has sufficient strength for screw implantation in terms of trabecular thickness and number, but weaker in terms of trabecular separation when compared with other carpal bones. Hamate has the greatest trabecular thickness among the other carpal bones, while it is ranked as the second in terms of trabecular number.

**Keywords:** carpal bones; hamate; micro-computed tomography; microstructure; trabeculae

Anatomy 2022;16(2):62–68 ©2022 Turkish Society of Anatomy and Clinical Anatomy (TSACA)

## Introduction

Hamate is a cuneiform bone with its special unciform process called as hook of hamate projecting from distal part of the palmar surface.<sup>[1]</sup> Hamate articulates with triquetrum, 4th and 5th metacarpal bones, and also with the ulnar side of the capitate. The hook of hamate projects from the volar side 1–2 cm distally and radially to the pisiform bone. It forms the ulnar side of the carpal tunnel and the radial side of Guyon's canal. Its ossification is not completed until the age of 15.<sup>[2]</sup> Several structures attach to the hook of hamate such as pisohamate ligament and transverse carpal ligament. Hamate is prone to subluxation and fractures because of its weak blood supply. Biomechanical factors, such as ligaments and muscles attaching to the bone can lead to fractures and subluxations. Blood supply may affect fracture healing (union-non-union procedure) and occurring avascular necrosis after trauma.<sup>[3]</sup>

Micro-computed tomography (Micro-CT) is a valuable method for the investigation of bone morphometry and microarchitecture. This method uses data sets obtained by

X-ray attenuation for the 3-dimensional representation of material density. In this era resolution of micro-CT devices has increased up to several micrometers.<sup>[4]</sup>

The literature reveals some pathological cases such as fractures,<sup>[5–8]</sup> avascular necrosis,<sup>[9–11]</sup> osteoblastoma,<sup>[12,13]</sup> osteochondroma,<sup>[14,15]</sup> and osteomyelitis<sup>[16]</sup> related to hamate. Hamate fractures occur in the body and hamulus parts of the bone. Both types of fractures are characterized by pain felt on the ulnar side of the wrist, which may be associated with ulnar paresthesia. Delayed diagnosis of the fracture may cause ulnar neuritis, ulnar artery thrombosis, and rupture of the flexor digitorum profundus tendons of 4th and 5th fingers.<sup>[17]</sup>

Clinical CT and micro-CT can be used to determine the bone microstructure. Studies have shown that all the values that can be measured with clinical CT can be measured more precisely with micro-CT. However, despite of the high resolution of micro-CT, its ability to scan only small parts that can be placed in its chamber makes it impossible to use it in a clinical setting.<sup>[18]</sup> This study

aimed to explore the trabecular microstructure of human dry hamates using micro-CT scanning method.

## Materials and Methods

Fifty-five human dry hamates without any external deformity were included in the study. The bones were obtained from collections of Anatomy Departments of Hacettepe and Ankara Universities in Turkey. Scanning and analysis were executed via micro-CT device (SkyScan 1174, SkyScan, Aartselaar, Belgium) at Hacettepe University. The scanning parameters were set as follows: degree of rotation=180°, exposure time=2700 milliseconds, current=800 mA, voltage=50 kVp, projection=33 µm and scanning time=90 minutes.

After the scanning procedure, the raw data in TIF format were reconstructed with Nrecon software (Micro Photonics Inc., Allentown, PA, USA) and axial images were generated in BMP format with 33 µm of projection. Then these reconstructed data were transferred to CTAn software and 2D–3D analysis was performed with this software. In this study we studied 2 groups of parameters; (i) volume-surface and (ii) trabecular properties. In the volume-surface group, we examined the following parameters: tissue volume, bone volume, percent bone volume (bone volume/tissue volume), bone surface, bone surface/volume ratio; while in the trabecular group we examined trabecular number, trabecular thickness, trabecular separation, structure model index and degree of anisotropy.

Statistical analysis was performed with IBM SPSS Statistics Version 23.0 (Armonk, NY, USA) with 95 % confidence interval. The distribution of variables (whether normally distributed or not) was tested via the Kolmogorov-Smirnov test.

## Results

The measurements were performed on 3D reconstruction images of the hamates (Figures 1 and 2). The average percentage of bone volume was  $44.930 \pm 5.859\%$ . There was high range in the average percentage of bone volume ranging between 29.65–60.78%. While the mean trabecular thickness was  $0.350 \pm 0.056$  mm, the average number of trabeculae for each mm was  $1.31 \pm 0.15$ . The average value for the trabecular separation, which indicates the mean space between trabeculae, was  $0.570 \pm 0.087$  mm. For trabecular number, trabecular thickness, and trabecular separation values, there was an up to two-fold difference between the minimum and maximum values (Table 1). While the samples showed a wide scatter in terms of structure-model index, the samples were much more homogeneous in terms of degree of anisotropy.

## Discussion

Bone strength is an important factor for implant treatment. This factor is related to bone integration. In some studies, a relationship is observed between bone quality and the success of implant treatment.<sup>[19,20]</sup> Bone mass, bone mineral density, macro and microarchitecture, and matrix properties are some of the factors which determine bone quality. Cortical bone is the primary determinant of bone robustness while the spongy bone is part of bone-implant integration. Information of trabecular bone structure has some importance for the success of implant treatment and further evaluation of implant surface architecture. Bone/implant integration is dependent upon the bone quality and bone/implant interphase.<sup>[21]</sup> Trabecular bone is the determinant of bone integration and forms the bone/implant interphase. For this reason, the trabecular bone structure should be researched to obtain objective and detailed scientific information. Lee et al.<sup>[22]</sup> scanned bones that had 4 different quality levels with the micro-CT device and revealed a statistically important relationship between bone quality and bone volume density, bone surface/volume ratio. Also, statistically significant correlations were observed between all the parameters. For this reason, in addition to trabecular parameters (trabecular thickness, number, and separation, structure-model index, degree of anisotropy) some other parameters (tissue volume, bone surface, bone volume, bone surface/volume ratio, percentage bone volume) which are affected by trabecular structure were also examined in the present study.

Tissue volume represents both volumes of bone tissue and spaces between these bone tissues while bone volume includes the only volume of bony structure but not spaces between these structures. Tissue volume and bone volume were observed as  $2526.120 \pm 604.615$  mm<sup>3</sup> and  $1137.100 \pm 318.973$  mm<sup>3</sup> subsequently in this study.

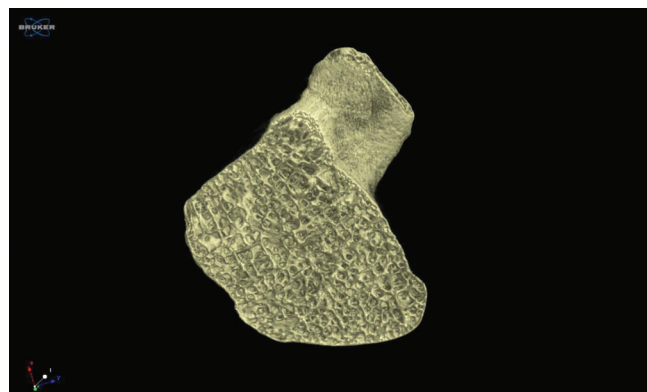
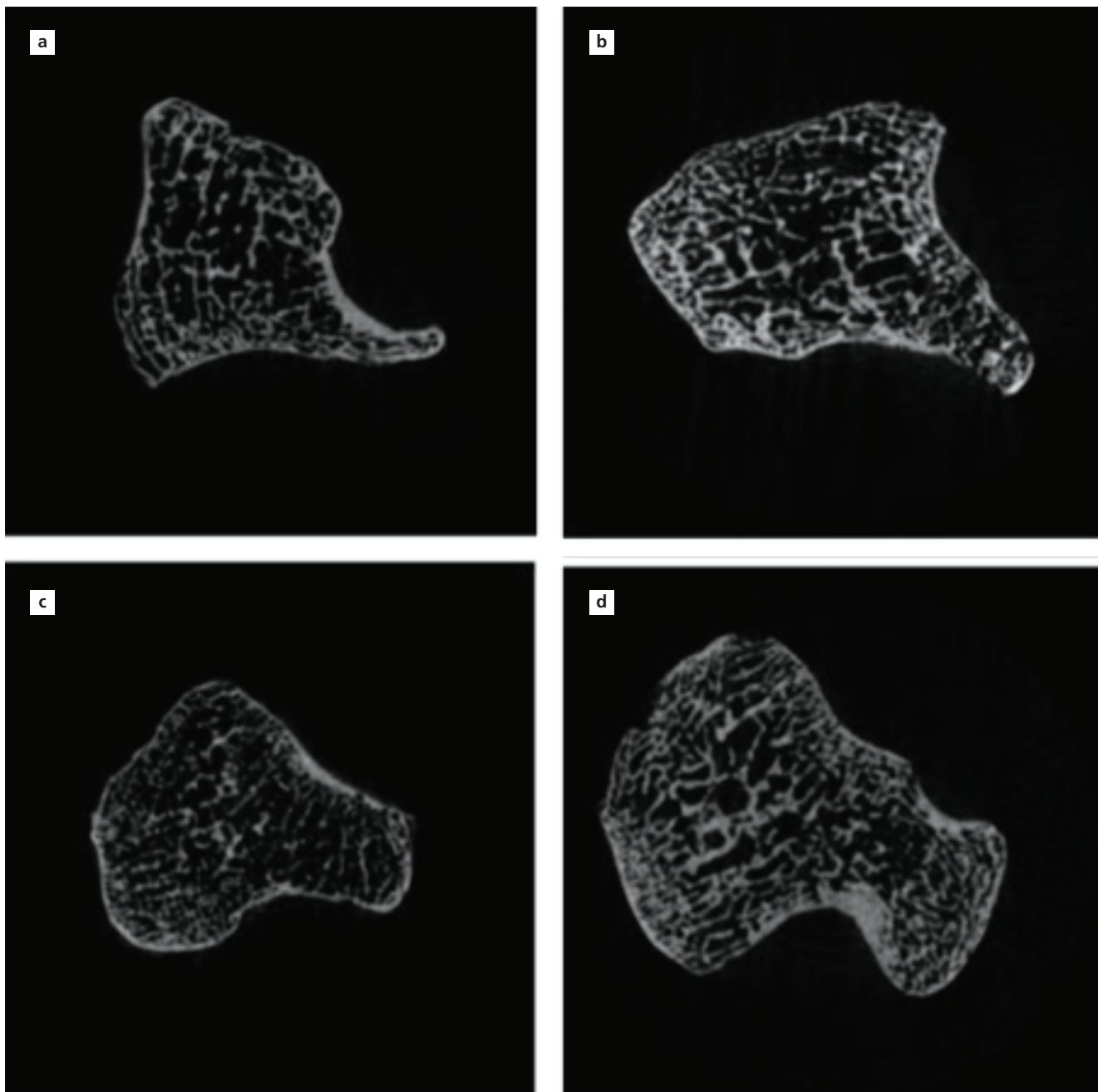


Figure 1. Trabecular structure of hamate.



**Figure 2.** Trabecular number, trabecular thickness, and trabecular separation of different hamates (a-d).

Percentage bone volume is the ratio of bone volume to tissue volume and was observed as  $44.930 \pm 5.859\%$  in our study. Previous studies have revealed data belonging to other carpal bones regarding bone and tissue volumes but since each carpal bone has a different dimension, it is quite an expected result that these bones will have different volume. So, it is not logical to compare these bones with each other in terms of volumes.

The bone surface represents the surface of trabeculae in inspected area. In our study the mean bone surface was measured as  $12149.250 \pm 3738.144 \text{ mm}^2$ . Trabecular number and thickness are parameters that change proportionately with the bone surface. Wurnig et al.<sup>[23]</sup> measured trabecular number and thickness as  $2.24 \pm 0.46 \text{ mm}^{-1}$  and  $0.229 \pm 0.032 \text{ mm}$  for cadaveric hamates. In our study, these values were  $1.31 \pm 0.150 \text{ mm}^{-1}$  and  $0.35 \pm 0.056 \text{ mm}$  for dry

**Table 1**

Results of the measurements (n=55).

|   | Mean±SD           | Min.–Max.        |
|---|-------------------|------------------|
| Tissue volume (mm <sup>3</sup> )              | 2526.12±604.615   | 1432.99–4358.62  |
| Bone volume (mm <sup>3</sup> )                | 1137.10±318.973   | 540.46–1987.47   |
| Percentage bone volume (%)                    | 44.93±5.859       | 29.65–60.78      |
| Bone surface (mm <sup>2</sup> )               | 12149.25±3738.144 | 6266.40–20443.43 |
| Bone surface/volume ratio (mm <sup>-1</sup> ) | 10.78±2.006       | 7.78–17.38       |
| Trabecular number (mm <sup>-1</sup> )         | 1.31±0.150        | 0.90–1.61        |
| Trabecular thickness (mm)                     | 0.35±0.056        | 0.23–0.49        |
| Trabecular separation (mm)                    | 0.57±0.087        | 0.38–0.83        |
| Structure-model index                         | -0.12±0.638       | -1.40–1.05       |
| Degree of anisotropy                          | 1.30±0.093        | 1.13–1.49        |

hamates subsequently. The bone surface/volume ratio represents the proportion of bone surface in the bone volume of the region of interest. Bone surface is also affected by trabecular number and thickness. In the aforementioned study<sup>[23]</sup> bone surface and bone surface/volume ratio parameters were not measured. Although it is not possible to judge the difference of the bone surface and bone surface/volume ratio with our study precisely, it is clear that none of these values (trabecular thickness and number) shows difference when compared with our study.

The trabecular number is the number of trabeculae that are observed in each mm of the sample. The higher number of trabeculae contributes positively to bone strength. We observed this value as  $1.310 \pm 0.150 \text{ mm}^{-1}$  while Wurnig et al.<sup>[23]</sup> as  $2.24 \pm 0.46 \text{ mm}^{-1}$ . In different studies, researchers compared normal carpal bones in various pathological conditions. Han et al.<sup>[24]</sup> compared normal lunates with those lunates which had Kienböck's disease, and they measured trabecular number as  $1.57 \pm 0.41 \text{ mm}^{-1}$  for normal lunates. Nufer et al.<sup>[25]</sup> studied normal trapezium and trapezium bones with osteoarthritis. The trabecular number was revealed as  $1.26 \pm 0.18 \text{ mm}^{-1}$  for non-pathological trapezium bones. Qu et al.<sup>[26]</sup> evaluated normal scaphoids and non-union scaphoids. They measured trabecular numbers for proximal and distal parts as  $0.08 \pm 0.04 \text{ mm}^{-1}$  and  $0.07 \pm 0.05 \text{ mm}^{-1}$  for normal specimens. It is known that bone strength changes proportionately with the trabecular number. Accordingly, it is possible to order the strength of the bones as lunate, hamate, trapezium, and scaphoid in terms of decreasing bone strength.

Trabecular thickness is the mean thickness of trabeculae in inspected area. Bone strength increases with higher trabecular thickness values. The trabecular thickness was

revealed as  $0.35 \pm 0.056 \text{ mm}$  in our study. Wurnig et al.<sup>[23]</sup> found this value as  $229 \pm 32 \mu\text{m}$  ( $0.229 \pm 0.032 \text{ mm}$ ) and Han et al.<sup>[24]</sup> as  $0.160 \pm 0.024 \text{ mm}$  for normal lunates. Nufer et al.<sup>[25]</sup> measured the trabecular thickness as  $0.17 \pm 0.02 \text{ mm}$  for normal trapezia; while Wurnig et al.<sup>[23]</sup> measured  $0.220 \pm 0.036 \text{ mm}$  for normal scaphoids. Increasing trabecular thickness is a factor that contributes to bone strength positively. When the bone strength is compared in terms of trabecular thickness the strength order will be in decreasing order as hamate, scaphoid, trapezium, and lunate.

Trabecular separation is a measure of the mean distance between trabeculae.<sup>[23]</sup> When trabecular number and thickness increase trabecular separation decreases and the behavior of these 3 parameters in this manner would increase the bone strength. In conclusion, the higher value of trabecular separation means the lower strength of the bone. In our study, the trabecular separation value was measured as  $0.57 \pm 0.087 \text{ mm}$ . Han et al.<sup>[24]</sup> revealed this value as  $0.52 \pm 0.21 \text{ mm}$  for lunates, Nufer et al.<sup>[25]</sup>  $0.74 \pm 0.18 \text{ mm}$  for trapezia, Qu et al.<sup>[26]</sup> as  $0.33 \pm 0.04 \text{ mm}$  (for proximal part) and  $0.33 \pm 0.05 \text{ mm}$  (for distal part) for scaphoids. In terms of trabecular separation, the bones can be ordered as the scaphoid, lunate, hamate, and trapezium in decreasing order of bone strength.

By the results of our study and other studies, it may be quite possible to judge differently when only one parameter is considered for determination of strength of the bone. For the diagnosis of some metabolic diseases such as osteoporosis and design of implant treatment for bone fractures, it is vital to consider multiple parameters to choose the correct treatment. And it is necessary to compare the results between samples whether they are statistically important or not.

Structure-model index is a trabeculae related factor. This factor may have -4, -3, 0, 3 and 4 values. “-4” and “-3” values correspond to spherical and cylindrical cavities while 0, 3 and 4 values represent smooth plate, cylindrical and spherical trabeculae. In our study, we measured the mean structure-model index as  $-0.12 \pm 0.638$ . These results indicate that our hamates had smooth plate-like trabeculae. Wurnig et al.<sup>[23]</sup> didn't study this parameter in their study. Han et al.<sup>[24]</sup> showed this value as  $1.99 \pm 0.31$  for normal lunates, Nufer et al.<sup>[25]</sup>  $1.35 \pm 0.44$  for normal trapezia and Qu et al.<sup>[26]</sup>  $0.63 \pm 0.74$  and  $0.63 \pm 1.00$  for proximal and distal parts of normal scaphoids. These results indicate that all the mentioned carpal bones together with hamate have smooth trabeculae. Change of structure-model index shows the changing pattern of trabeculae. For instance, Qu et al.<sup>[26]</sup> compared normal scaphoids with non-union scaphoids and observed that the latter has a higher value of structure-model index at its distal part. They also observed that the trabecular shape of the distal part resembled a cylinder in contrast to the proximal part's trabeculae. However, proximal part has a lower SMI showing its plate-like appearance, which is also an indicator of dense trabecular structure and stronger bone. The plate-like trabecular structure is a result of higher mechanical stress while the cylindrical shape is a result of lower mechanical stress. In conclusion, it can be said that hamates may be exposed to high mechanical stress.

Degree of anisotropy is a representation of trabecular distribution in the region of interest. If it is equal to 1 it means an isotropic trabecular distribution (alignment along the same axes) exists but values greater than 1 show anisotropic distribution. In this study, this value is measured as  $1.30 \pm 0.093$ . This result shows us that our hamate samples have an anisotropic trabeculae distribution. Wurnig et al.<sup>[23]</sup> measured this value as  $1.56 \pm 0.08$ . In previous studies, degree of anisotropy was revealed as  $0.44 \pm 0.86$  for lunates<sup>[24]</sup> and  $1.28 \pm 0.04$  for trapezia.<sup>[25]</sup> Accordingly, we can conclude that hamates and trapezia have an anisotropic trabeculae distribution in contrast to lunates which have an isotropic distribution. The degree of anisotropy is a measure of bone adaptation to the changing conditions of the structure-model index. For instance, Han et al.<sup>[24]</sup> observed that in the case of progressing bone necrosis, nonnecrotic bony tissue changes its trabecular distribution towards anisotropic in response to compressive stress. So, it is important to be aware of changing pattern of trabecular distribution due to different conditions.

Bone quality is so important for screw implantation and lower bone quality affects screw stability in a negative

manner.<sup>[27]</sup> For this reason, it is vital to evaluate the trabecular structure that has important effects on bone quality and strength. It is stated that the bone reorganizes its trabecular structure as a response to increasing force load in the affected region.<sup>[28]</sup> Accordingly, a carpal bone with an inner position, attached structures (muscles, ligaments, etc.), and microarchitecture would respond to different physiological and pathological conditions in a special manner. So, each bone should be evaluated by considering its position relative to other bones. For instance Mc Lean et al.<sup>[29]</sup> observed 2 types of distinct joints between triquetrum and hamate which were named as TqH-1 and TqH-2 respectively depending on articular surfaces of triquetrum and hamate. In another study, it was revealed that depending on the joint surfaces of triquetrum and hamate, a rotational motion occurs instead of helicoidal movement that refers to a saddle joint.<sup>[30]</sup> So in addition to anatomical properties, functional properties should be considered for any medical intervention on carpal bones. In addition to relative positions of the carpal bones, the intrinsic structural dynamics of individual bones should also be evaluated for a proper localization of screws. For instance, in a study documenting the differences of bone volume-surface and trabecular properties between different quadrants of scaphoid bone, no differences in terms of bone quality and density between these 4 quadrants was noted.<sup>[31]</sup> The vascular supply of the carpal bones is another factor affecting the healing process. Hamate is noted to have two regions of vascular entry and without intraosseous anastomoses. This type of vascular supply pattern puts hamate in a low risk group for developing avascular necrosis.<sup>[32]</sup> Another factor that might have a role in healing process could be the bone age. The analysis of images obtained by CT of the carpal bones is a valid method in the evaluation of bone maturity in children. Choi et al.<sup>[33]</sup> stated that capitohamate (CH) planimetry could be a reliable method for determining bone age. Determining the normal anatomy of the carpal bones will also help to determine the most appropriate parameters in the clinic for treating wrist pathologies.<sup>[33-35]</sup>

Our aim in this study was to define the trabecular structure of hamate, which is one of the parameters affecting the bone strength. Trabecular number, thickness, separation, structure-model index, and degree of anisotropy can be regarded among other factors. Examining only the dry bones and inability to identify the age and genders of the samples are two big limitations of our study. Therefore, we suggest carrying out new studies comparing dry bones with cadaveric specimens and trabecular structure changes in different pathological conditions together with the vasculature of hamate.

## Conclusion

It is obvious that hamate bone has sufficient strength for screw implantation in terms of trabecular thickness and number, but weaker in terms of trabecular separation when compared with other carpal bones. Hamate has the greatest trabecular thickness among the other carpal bones, while it is ranked as the second in terms of trabecular number. In terms of trabecular separation, the carpal bones can be ordered as the scaphoid, lunate, hamate, and trapezium in decreasing order of bone strength.

## Conflict of Interest

The authors declare no conflict of interest.

## Author Contributions

HO: protocol/project development, data collection, data analysis, manuscript writing/editing; HHC: supervision; MO: data collection, data analysis; FG: data collection, data analysis.

## Ethics Approval

The study was approved by Ethical Committee of Hacettepe University (No: GO 18/131-12) and performed in accordance with the Helsinki declaration of principles.

## Funding

The authors declare no financial support.

## References

- Ross CA. Wrist and hand. In: Standring S, editor. *Gray's anatomy: the anatomical basis of clinical practice*. 41st ed. Edinburgh (Scotland): Elsevier Churchill Livingstone; 2016. p. 869.
- Walsh JJ 4th, Bishop AT. Diagnosis and management of hamate hook fractures. *Hand Clin* 2000;16:397-403.
- Foucher G, Schuind F, Merle M, Brunelli F. Fractures of the hook of the hamate. *J Hand Surg Br* 1985;10:205-10.
- Boussein ML, Boyd SK, Christiansen BA, Guldberg RE, Jepsen KJ, Müller R. Guidelines for assessment of bone microstructure in rodents using micro-computed tomography. *J Bone Miner Res* 2010; 25:1468-86.
- De Schrijver F, De Smet L. Fracture of the hook of the hamate, often misdiagnosed as "wrist sprain". *J Emerg Med* 2001;20:47-51.
- Evans MW. Hamate hook fracture in a 17-year-old golfer: importance of matching symptoms to clinical evidence. *J Manipulative Physiol Ther* 2004;27:516-8.
- Cano Gala C, Pescador Hernández D, Rendón Díaz DA, López Olmedo J, Blanco Blanco J. Fracture of the body of hamate associated with a fracture of the base of fourth metacarpal: A case report and review of literature of the last 20 years. *Int J Surg Case Rep* 2013;4: 442-5.
- How Kit N, Malherbe M, Hulet C. Hamate hook stress fracture in a professional bowler: case report of an unusual causal sport. *Hand Surg Rehabil* 2017;36:62-5.
- Van Demark RE, Parke WW. Avascular necrosis of the hamate: a case report with reference to the hamate blood supply. *J Hand Surg Am* 1992;17:1086-90.
- De Smet L. Avascular necrosis of multiple carpal bones. A case report. *Chir Main* 1999;18:202-4.
- Peters SJ, Verstappen C, Degreef I, Smet LD. Avascular necrosis of the hamate: three cases and review of the literature. *J Wrist Surg* 2014;3:269-74.
- van Dijk M, Winters HA, Wuisman PI. Recurrent osteoblastoma of the hamate bone. A two-stage reconstruction with a free vascularized iliac crest flap. *J Hand Surg Br* 1999;24:501-5.
- Gdoura F, Trigui M, Ellouze Z, Hamed YB, Ayadi K, Keskes H. Hamatum osteoblastoma. *Orthop Traumatol Surg Res* 2010;96: 712-6.
- Ayan I, Serinsöz E. Osteoblastoma in the os hamatum: a rare case report. [Article in Turkish] *Eklemler Hastalıkları Cerrahisi* 2014;25:56-9.
- Koti M, Honakeri SP, Thomas A. A multilobed osteochondroma of the hamate: case report. *J Hand Surg Am* 2009;34:1515-7.
- Cha SM, Shin HD, Kim DY. A solitary unilobed osteochondroma of the hamate: a case report. *J Pediatr Orthop B* 2017;26:274-6.
- Santoshi JA, Pallapati SC, Thomas BP. Haematogenous pseudomonas osteomyelitis of the hamate--treatment by radical debridement and bone grafting. *J Plast Reconstr Aesthet Surg* 2010;63:189-90.
- Geneci F, Denk CC, Uzuner MB, Ocak M, Doğan İ, Sayacı EY, Gürses İA, Çay N, Baykal D, Çelik HH, Cömert A. Morphometric evaluation of coccyx with microcomputed tomography (micro CT) and computed tomography (CT) technology. *Journal of Innovative Approaches in Medicine* 2022;3:1-19.
- Jemt T, Lekholm U. Oral implant treatment in posterior partially edentulous jaws: a 5-year follow-up report. *Int J Oral Maxillofac Implants* 1993;8:635-40.
- Drago CJ. Rates of osseointegration of dental implants with regard to anatomical location. *J Prosthodont* 1992;1:29-31.
- Puleo DA, Nanci A. Understanding and controlling the bone-implant interface. *Biomaterials* 1999;20:2311-21.
- Lee JH, Kim HJ, Yun JH. Three-dimensional microstructure of human alveolar trabecular bone: a micro-computed tomography study. *J Periodontal Implant Sci* 2017;47:20-9.
- Wurnig MC, Calcagni M, Kenkel D, Vich M, Weiger M, Andreisek G, Wehrli FW, Boss A. Characterization of trabecular bone density with ultra-short echo-time MRI at 1.5, 3.0 and 7.0 T - comparison with micro-computed tomography. *NMR Biomed* 2014;27:1159-66.
- Han KJ, Kim JY, Chung NS, Lee HR, Lee YS. Trabecular microstructure of the human lunate in Kienbock's disease. *J Hand Surg Eur Vol* 2012;37:336-41.
- Nufer P, Goldhahn J, Kohler T, Kuhn V, Müller R, Herren DB. Microstructural adaptation in trapezium bone due to subluxation of the thumb. *J Orthop Res* 2008;26:208-16.
- Qu G, von Schroeder HP. Trabecular microstructure at the human scaphoid nonunion. *J Hand Surg Am* 2008;33:650-5.
- Alonso-Vázquez A, Lauge-Pedersen H, Lidgren L, Taylor M. The effect of bone quality on the stability of ankle arthrodesis. A finite element study. *Foot Ankle Int* 2004;25:840-50.
- Wolff J. *Das Gesetz der Transformation der Knochen*. Berlin: Hirschwald; 1892. p. 281.
- McLean J, Bain G, Eames M, Fogg Q, Pourgiez N. An anatomic study of the triquetrum-hamate joint. *J Hand Surg Am* 2006;31: 601-7.

30. Moritomo H, Goto A, Sato Y, Sugamoto K, Murase T, Yoshikawa H. The triquetrum-hamate joint: an anatomic and in vivo three-dimensional kinematic study. *J Hand Surg Am* 2003;28:797–805.
31. Huntington LS, Mandaleson A, Hik F, Ek ETH, Ackland DC, Tham SKY. Measurement of scaphoid bone microarchitecture: a computed tomography imaging study and implications for screw placement. *J Hand Surg Am* 2020;45:1185.e1-1185.e8.
32. Panagis JS, Gelberman RH, Taleisnik J, Baumgaertner M. The arterial anatomy of the human carpus. Part II: the intraosseous vascularity. *J Hand Surg Am* 1983;8:375–82.
33. Choi A, Kim YC, Min SJ, Khil EK. A simple method for bone age assessment: the capitohamate planimetry. *European Radiol* 2018;28:2299–307.
34. Canovas F, Roussanne Y, Captier G, Bonnel F. Study of carpal bone morphology and position in three dimensions by image analysis from computed tomography scans of the wrist. *Surg Radiol Anat* 2004;26:186–90.
35. Canovas F, Banegas F, Cyteval C, Jaeger M, DiMéglio A, Bonnel F, Sultan C. Carpal bone maturation assessment by image analysis from computed tomography scans. *Horm Res* 2000;54:6–13.

**ORCID ID:**

H. Ocak 0000-0002-0288-4167;  
H. H. Çelik 0000-0002-7909-7604;  
M. Ocak 0000-0001-6832-6208;  
F. Geneci 0000-0002-5039-4664



**Correspondence to:** Hakan Ocak, PhD

Department of Anatomy, Faculty of Medicine,  
Ağrı İbrahim Çeçen University, Ağrı, Türkiye  
Phone: +90 553 608 89 13  
e-mail: hocak@agri.edu.tr

*Conflict of interest statement:* No conflicts declared.

This is an open access article distributed under the terms of the Creative Commons Attribution-NonCommercial-NoDerivs 4.0 Unported (CC BY-NC-ND4.0) Licence (<http://creativecommons.org/licenses/by-nc-nd/4.0/>) which permits unrestricted noncommercial use, distribution, and reproduction in any medium, provided the original work is properly cited. *How to cite this article:* Ocak H, Çelik HH, Ocak M, Geneci F. Evaluation of trabecular structure of hamate using micro-computed tomography. *Anatomy* 2022;16(2):62–68.